

## Flow in Collapsible Tubes with Discontinuous Mechanical Properties: Mathematical Model and Exact Solutions

Eleuterio F. Toro<sup>1</sup> and Annunziato Siviglia<sup>1,\*</sup>

<sup>1</sup> *Laboratory of applied Mathematics, University of Trento, Via Mesiano 77, I-38100 Trento, Italy.*

Received 21 June 2011; Accepted (in revised version) 24 February 2012

Communicated by Chi-Wang Shu

Available online 28 June 2012

---

**Abstract.** We formulate a one-dimensional time-dependent non-linear mathematical model for some types of physiological fluid flow in collapsible tubes with discontinuous material properties. The resulting  $6 \times 6$  hyperbolic system is analysed and the associated Riemann problem is solved exactly. Although the solution algorithm deals with idealised cases, it is nonetheless uniquely well-suited for assessing the performance of numerical methods intended for simulating more general situations. Moreover, our model may be a useful starting point for numerical calculations of realistic flows involving rapid and discontinuous material property variations. One important example in mind is the simulation of blood flow in medium-to-large veins in humans. Finally, we also discuss some peculiarities of the model regarding the loss of strict hyperbolicity and uniqueness. In particular we show an example in which the solution of the Riemann problem is non unique.

**AMS subject classifications:** 76Z05

**Key words:** Collapsible tubes, physiological flows, blood flows, Riemann problem.

---

## 1 Introduction

The theoretical study of flow phenomena in humans through mathematical models is closely related to the study of flow of an incompressible liquid in thin-walled collapsible tubes. In fact the applicability of theoretical models for thin-walled collapsible tubes covers a wider variety of physiological phenomena as well the design of clinical devices for practical medical applications. Fluid flow through compliant tubes is usually used

---

\*Corresponding author. *Email addresses:* toroe@ing.unitn.it (E. F. Toro), nunzio.siviglia@ing.unitn.it (A. Siviglia)

to represent physiological flows such as blood flow in arteries and veins, air flow in the airways and urine flow in the ureter. In this paper we are interested in theoretical models for determining flow patterns and the geometry of the tube by the interaction between the flexible wall of the tube and internal flow. We centre our attention on one-dimensional, time-dependent non-linear models. Classical works on this subject are, for example, [21], [28], and the many references therein. For more recent works see [2, 7, 10, 12, 13, 29, 31].

This paper is motivated by physical situations of medical interest in which certain properties that characterize compliant vessels, external pressures and body forces change rapidly, or even discontinuously. Physical quantities of interest are vessel wall thickness, equilibrium cross sectional area and Young's modulus. Prominent examples arise in the surgical treatment of Abdominal Aortic Aneurysms [35] that includes the insertion of stents. Stents are also implanted in veins [1] and in the ureter [6] in different circumstances. These devices do not always match the compliance properties of natural vessels and discontinuous jumps of physical properties may arise, influencing significantly the wave propagation phenomena associated with the fluid dynamics. External pressures and body forces are another source of potentially rapid or even discontinuous variations, which again will influence the wave phenomenon [21]. Here we formulate a mathematical model that allows for the discontinuous variations of certain vessel properties, all in the context of simplified one-dimensional flow. In spite of the very strong assumptions, we still expect the one-dimensional model to provide by itself useful information for practical purposes. Moreover, one-dimensional models are an integral part of large models in multiscale approaches [29] and thus the present work may also be useful in the construction of more realistic models.

In current models used for numerical simulation of blood flow phenomena the effect of the variation of the above mentioned quantities enters the equations in the form of source terms; see [31], for example. In particular, for external forces such as muscle forces, the corresponding source term involves a pressure gradient source term, analogous to the geometric source term given by bottom variation in shallow water models [32]. In the numerical analysis literature it is well known that such source terms are likely to cause serious numerical difficulties. An important issue is the construction *well balanced schemes* that achieve equilibrium between advective and source terms in the equations near the steady state [18, 23, 27]. The severity of the numerical difficulties increases as spatial gradients of the physical quantities of interest increase.

In this paper we formulate and study a simplified model in which discontinuities of three parameters are permitted, namely wall thickness, Young's modulus and cross sectional area at rest. Moreover we add two extra equations, one for the time variation of the external pressure  $p_e$  and one for the transport of a passive scalar. We study the mathematical properties of the resulting  $6 \times 6$  hyperbolic system and obtain the exact solution of the associated Riemann problem. Exact solutions constitute reference solutions for assessing the performance of numerical methods intended for general use. Some preliminary results, obtained using a simpler model with one extra equation, have already been published [34]. Potentially, the proposed formulation would facilitate the numeri-

cal treatment of source terms due to spatial variation of material properties and external forces. There are, however, two major difficulties with our formulation, namely the potential occurrence of *resonance* [19,24] and the loss of uniqueness, see [4]. These issues are currently the subject of further studies by the authors and collaborators; results will be published elsewhere.

In summary, this paper presents a mathematical model for blood flow in medium to large arteries and veins in which rapid or even discontinuous variations of vessel properties are permitted. Exact solutions of the equations are presented for special cases, which may turn to be useful for assessing numerical solutions to the more general initial boundary value problem. Both the model and the solution to the Riemann problem presented constitute a building block for realistic computations of practical value, which will be the subject of future communications.

The rest of the paper is structured as follows. In Section 2 we review the governing equations and the tube law to be used. In Section 3 we introduce and study a  $6 \times 6$  hyperbolic model with discontinuous property variations. In Section 4 we formulate and solve exactly the Riemann problem. In Section 5 we show sample exact solutions. In Section 6 we discuss the problem related to non-uniqueness and show one example where it occurs. Conclusions are drawn in Section 7.

## 2 Mathematical model

Consider the geometric situation described in Fig. 1, which depicts a model for a blood vessel. The mathematical model will assume one-dimensional flow in the axial direction  $x$ .

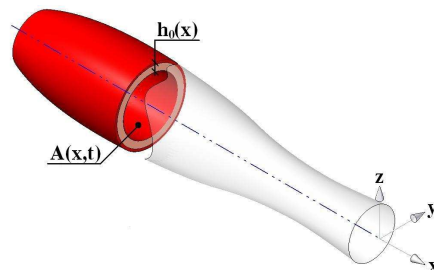


Figure 1: Assumed axially symmetric vessel configuration in three space dimensions at time  $t$ . Cross sectional area  $A(x,t)$  and wall thickness  $h_0(x)$  are illustrated.

### 2.1 Basic relations and quantities

The basic equations for the flow of blood in medium-size to large arteries and veins are obtained from the principles of conservation of mass

$$\partial_t A + \partial_x (uA) = 0 \quad (2.1)$$

and momentum

$$\partial_t(uA) + \partial_x(\hat{\alpha}Au^2) + \frac{A}{\rho}\partial_x p = -Ru. \quad (2.2)$$

$A(x,t)$  is the cross-sectional area of the vessel or tube at position  $x$  and time  $t$ ,  $u(x,t)$  is the averaged velocity of blood at a cross section,  $p(x,t)$  is pressure,  $\rho$  is the density of blood, assumed constant, and  $R > 0$  is the viscous resistance of the flow per unit length of the tube, assumed to be a known function. We assume  $\hat{\alpha} = 1$  in the momentum equation (2.2).

There are two governing partial differential equations (2.1)-(2.2), and three unknowns, namely  $A(x,t)$ ,  $u(x,t)$  and  $p(x,t)$ . An extra relation is required to close the system. This is provided by the *tube law*, which relates the pressure  $p(x,t)$  to the wall displacement via the cross-sectional area  $A(x,t)$ . The tube law couples the elastic properties of the vessel to the fluid dynamics and is analogous to the *equation of state* in gas dynamics [33].

## 2.2 Tube law

Here we adopt a tube law of the form

$$p = p_e(x,t) + \psi(A; A_0, K), \quad (2.3)$$

where

$$\psi(A; A_0, K) = p - p_e \equiv p_{trans} \quad (2.4)$$

is the *transmural pressure*, the difference between the pressure in the vessel, the *internal pressure*, and the external pressure. Here we choose [14]

$$\psi(A; A_0, K) = K(x)[\alpha^m - \alpha^n], \quad \text{with } \alpha = \frac{A}{A_0}, \quad (2.5)$$

where

$$K(x) = \frac{E(x)}{12(1-\nu^2)} \left( \frac{h_0(x)}{R_0(x)} \right)^3. \quad (2.6)$$

Here  $h_0(x)$  is the vessel thickness;  $A_0(x)$  and  $R_0(x)$  are the cross-sectional area of the vessel and the radius at equilibrium;  $p_{trans} = 0$ ;  $E(x)$  is the Young's modulus;  $\nu$  is the Poisson ratio and  $m \geq 0$  and  $n \leq 0$  are real numbers. The external pressure  $p_e$ , assumed to be known, may be decomposed as follows

$$p_e(x,t) = p_{atm} + p_{musc}(x,t), \quad (2.7)$$

where  $p_{atm}$  is the atmospheric pressure, assumed constant here, and  $p_{musc}(x,t)$  is the pressure exerted by the surrounding tissue, assumed to be a prescribed function of both position and time. See [36] for a discussion on  $p_{musc}(x,t)$  in the context of chronic venous disease and see [25] for a discussion on external tissue forces when studying a portion of the arterial tree. For a fuller discussion on tube laws see, for example, [7, 13, 14, 28, 29].

### 3 Model for discontinuous properties

In this section we reformulate the mathematical model (2.1)-(2.6) so as to accommodate discontinuous variations of material properties such as Young's modulus, equilibrium cross-sectional area and wall thickness.

#### 3.1 Equations

We consider a mathematical model consisting of the partial differential equations (2.1)-(2.2), along with the tube law (2.3)-(2.5). We assume wall thickness  $h_0(x)$ , equilibrium cross-sectional area  $A_0(x)$  and Young's modulus  $E(x)$  to be functions of axial distance  $x$ . Then the pressure gradient in (2.2) is

$$\partial_x p = \psi_A \partial_x A + \psi_K \partial_x K + \psi_{A_0} \partial_x A_0 + \partial_x p_e(x, t), \quad (3.1)$$

with

$$\psi_A = \frac{\partial \psi}{\partial A} = \frac{K}{A} [m\alpha^m - n\alpha^n], \quad (3.2)$$

$$\psi_K = \frac{\partial \psi}{\partial K} = \alpha^m - \alpha^n, \quad (3.3)$$

$$\psi_{A_0} = \frac{\partial \psi}{\partial A_0} = -\frac{K}{A_0} [m\alpha^m - n\alpha^n]. \quad (3.4)$$

The complete system reads

$$\begin{cases} \partial_t A + \partial_x (uA) = 0, \\ \partial_t (uA) + \partial_x (Au^2) + \frac{A}{\rho} \psi_A \partial_x A = -\frac{A}{\rho} \psi_K \partial_x K - \frac{A}{\rho} \psi_{A_0} \partial_x A_0 - \frac{A}{\rho} \partial_x p_e(x, t) - Ru. \end{cases} \quad (3.5)$$

We note that the principal part of the equations (left-hand side) does not have conservation-law form. Note also that there are source terms on the right hand side which depend on gradients of the vessel properties  $E(x)$ ,  $A_0(x)$ , and  $h_0(x)$  and the external pressure. The external pressure  $p_e(x, t)$  is analogous to bottom variation in shallow water flows [32], both giving rise to a source term involving a spatial gradient. In the rest of this paper we assume

$$\partial_t (p_e) = F(x, t), \quad (3.6)$$

where  $F(x, t)$  is a prescribed function of space and time. In the numerical literature it is well known that the treatment of such source terms, sometimes known as *geometric source terms*, is notoriously difficult. Common difficulties include the generation of spurious oscillations and the lack of balance between convective terms and source terms in the steady state. For a discussion on these issues see, for example, [18, 23, 27] and references

therein. In principle, for slowly-varying vessel properties one can still proceed with formulation (3.5). However, for significant vessel property variations, or even in the case of discontinuous properties, formulation (3.5) is not suitable.

In this paper we present an alternative formulation of the model by considering the variable vessel properties  $A_0(x)$ ,  $h_0(x)$  and  $E(x)$  as additional unknowns of the problem [16–18,22]. We then add the following obvious partial differential equations

$$\partial_t K(x) = 0, \quad \partial_t A_0(x) = 0. \quad (3.7)$$

It is worth noting that the first equation also includes spatial variations of  $h_0$ . A possible extension to this basic model could be obtained by considering one additional equation to account for the concentration  $\phi(x,t)$  of one quantity passively transported with the fluid speed  $u(x,t)$ . For real applications this variable (or many of them) may be very useful in the modelling of transport of chemicals in the flow. From the mathematical point of view it is sufficient to consider one concentration variable here. We then combine the advection equation for  $\phi$  with the continuity equation to obtain the following advection equation in conservative form:

$$\partial_t (A\phi) + \partial_x (Au\phi) = 0. \quad (3.8)$$

The enlarged system from (3.5) and (3.8) in quasi-linear form reads

$$\partial_t \mathbf{Q} + \mathbf{A}(\mathbf{Q}) \partial_x \mathbf{Q} = \mathbf{S}(\mathbf{Q}), \quad (3.9)$$

where

$$\mathbf{Q} = \begin{bmatrix} q_1 \\ q_2 \\ q_3 \\ q_4 \\ q_5 \\ q_6 \end{bmatrix} \equiv \begin{bmatrix} A \\ Au \\ K \\ A_0 \\ p_e \\ A\phi \end{bmatrix}, \quad \mathbf{S}(\mathbf{Q}) = \begin{bmatrix} s_1 \\ s_2 \\ s_3 \\ s_4 \\ s_5 \\ s_6 \end{bmatrix} \equiv \begin{bmatrix} 0 \\ -Ru \\ 0 \\ 0 \\ F(x,t) \\ 0 \end{bmatrix}, \quad (3.10)$$

$$\mathbf{A}(\mathbf{Q}) = \begin{bmatrix} 0 & 1 & 0 & 0 & 0 & 0 \\ \frac{A}{\rho} \psi_A - u^2 & 2u & \frac{A}{\rho} \psi_K & \frac{A}{\rho} \psi_{A_0} & \frac{A}{\rho} & 0 \\ 0 & 0 & 0 & 0 & 0 & 0 \\ 0 & 0 & 0 & 0 & 0 & 0 \\ 0 & 0 & 0 & 0 & 0 & 0 \\ -u\phi & \phi & 0 & 0 & 0 & u \end{bmatrix}. \quad (3.11)$$

Next we study some mathematical properties of the equations.

### 3.2 Eigenstructure and characteristic fields

The eigenstructure of the first-order system (3.9)-(3.11) is that of the principal part of the system (source terms ignored) and is given by the eigenvalues and corresponding eigenvectors.

**Proposition 3.1.** The eigenvalues of the homogeneous version of (3.9) are all real and given by

$$\lambda_1 = u - c, \quad \lambda_2 \equiv \lambda_3 \equiv \lambda_4 = 0, \quad \lambda_5 = u \quad \lambda_6 = u + c, \tag{3.12}$$

where

$$c = \sqrt{\frac{A}{\rho} \psi_A} = \sqrt{\frac{K}{\rho} [m\alpha^m - n\alpha^n]} \tag{3.13}$$

is the *wave speed*.

Note that the wave speed  $c$  is analogous to the *sound speed in gas dynamics* [33] and to the celerity in shallow water flows [32]. Note also that the choice  $m \geq 0$  and  $n \leq 0$  for the coefficients of the tube law, make the wave speed  $c$  always real.

*Proof.* By definition the eigenvalues of system (3.9)-(3.10) are the eigenvalues of the matrix  $\mathbf{A}$ , which in turn are the roots of the characteristic polynomial

$$P(\lambda) = \text{Det}(\mathbf{A} - \lambda \mathbf{I}) = 0, \tag{3.14}$$

where  $\mathbf{I}$  is the identity matrix and  $\lambda$  is a parameter. Simple calculations give

$$P(\lambda) = \lambda^3 (\lambda^2 - 2u\lambda + u^2 - c^2) (u - \lambda) = 0,$$

from which the result (3.12) follows. □

**Proposition 3.2.** The right eigenvectors of  $\mathbf{A}$  corresponding to the eigenvalues (3.12) are

$$\mathbf{R}_1 = \gamma_1 \begin{bmatrix} 1 \\ u - c \\ 0 \\ 0 \\ 0 \\ \phi \end{bmatrix}, \quad \mathbf{R}_2 = \gamma_2 \begin{bmatrix} 0 \\ 0 \\ 1 \\ 0 \\ -\psi_K \\ 0 \end{bmatrix}, \quad \mathbf{R}_3 = \gamma_3 \begin{bmatrix} 0 \\ 0 \\ 0 \\ 1 \\ -\psi_{A_0} \\ 0 \end{bmatrix}, \tag{3.15}$$

$$\mathbf{R}_4 = \gamma_4 \begin{bmatrix} 1 \\ 0 \\ 0 \\ 0 \\ \frac{\rho}{A}(u^2 - c^2) \\ \phi \end{bmatrix}, \quad \mathbf{R}_5 = \gamma_5 \begin{bmatrix} 0 \\ 0 \\ 0 \\ 0 \\ 0 \\ 1 \end{bmatrix}, \quad \mathbf{R}_6 = \gamma_6 \begin{bmatrix} 1 \\ u + c \\ 0 \\ 0 \\ 0 \\ \phi \end{bmatrix}, \tag{3.16}$$

where  $\gamma_i$ , for  $i = 1, \dots, 6$ , are arbitrary scaling factors.

*Proof.* For an arbitrary right eigenvector  $\mathbf{R} = [r_1, r_2, r_3, r_4, r_5, r_6]^T$  we have

$$\mathbf{A}\mathbf{R} = \lambda\mathbf{R}, \tag{3.17}$$

which gives the algebraic system

$$\begin{cases} r_2 = \lambda r_1, \\ (c^2 - u^2)r_1 + 2ur_2 + \frac{A}{\rho}\psi_K r_3 + \frac{A}{\rho}\psi_{A_0} r_4 + \frac{A}{\rho}r_5 = \lambda r_2, \\ 0 = \lambda r_3, \\ 0 = \lambda r_4, \\ 0 = \lambda r_5, \\ -u\phi r_1 + \phi r_2 + ur_6 = \lambda r_6. \end{cases} \tag{3.18}$$

By substituting  $\lambda$  in (3.18) by the appropriate eigenvalues in (3.12) in turn we arrive at the sought result.  $\square$

**Proposition 3.3.** The  $\lambda_1$  and  $\lambda_6$  characteristic fields are genuinely non-linear outside the locus

$$\mathcal{G}\left(m, n, \frac{A}{A_0}\right) = m(m+2)\alpha^m - n(n+2)\alpha^n$$

in the  $m - n - \alpha$  space, and the  $\lambda_i$ -characteristic fields, for  $i = 2, \dots, 5$ , are linearly degenerate.

*Proof.* Since  $\lambda_i = 0$  for  $i = 2, 3, 4$  it follows that  $\nabla \lambda_i = \mathbf{0}$  and thus  $\nabla \lambda_i \cdot \mathbf{R}_i = 0$ . Therefore the  $\lambda_i$ -characteristic fields, for  $i = 2, 3, 4$ , are linearly degenerate as claimed. For the fifth characteristic field  $\lambda_5 = u$ ,  $\nabla \lambda_5 \cdot \mathbf{R}_5 = 0$  and thus the field is linearly degenerate as claimed.

For the other two characteristic fields, some algebraic manipulations give

$$\nabla \lambda_1 \cdot \mathbf{R}_1 = -\nabla \lambda_6 \cdot \mathbf{R}_6 = \frac{K[m(m+2)\alpha^m - n(n+2)\alpha^n]}{2A\sqrt{\rho K[m\alpha^m - n\alpha^n]}}.$$

Therefore the  $\lambda_1(\mathbf{Q})$  and  $\lambda_6(\mathbf{Q})$  characteristic fields are genuinely non-linear provided  $m(m+2)\alpha^m \neq n(n+2)\alpha^n$ . For the usual cases in which  $m \geq 0$  and  $n \geq -2$  (see [7, 10]) the two characteristic fields are genuinely non-linear, and the proof is complete.  $\square$

### 3.3 Generalized Riemann invariants

The generalized Riemann invariants are relations that are valid across simple waves. These are most conveniently expressed as a set of ordinary differential equations in phase space, see [20] for details.

**Proposition 3.4.** For a given hyperbolic system of  $s$  unknowns  $[w_1, w_2, \dots, w_s]^T$ , for any  $\lambda_i$ -characteristic field with right eigenvector  $\mathbf{R}_i = [r_{1i}, r_{2i}, \dots, r_{si}]^T$  the generalized Riemann invariants are solutions of the following  $s - 1$  ordinary differential equations in phase space

$$\frac{dw_1}{r_{1i}} = \frac{dw_2}{r_{2i}} = \dots = \frac{dw_s}{r_{si}}. \tag{3.19}$$

*Proof.* Omitted, see [20].  $\square$

**Proposition 3.5.** The generalized Riemann invariants for  $\lambda_1 = u - c$  are

$$A_0 = \text{const}, \quad K = \text{const}, \quad p_e = \text{const}, \quad \phi = \text{const}, \quad \int \frac{c(A)}{A} dA + u = \text{const}. \quad (3.20)$$

*Proof.* Application of Eq. (3.19) from Proposition 3.4 to  $\lambda = \lambda_1 = u - c$  with  $\mathbf{R}_1 = \gamma_1 [1, u - c, 0, 0, 0, 0]^T$ , with  $\gamma_1 = 1$  give

$$\frac{dA}{1} = \frac{d(Au)}{u - c} = \frac{dK}{0} = \frac{dA_0}{0} = \frac{dp_e}{0} = \frac{dA\phi}{\phi}. \quad (3.21)$$

The third, fourth and fifth members of the 5 equalities in (3.21) give the first sought results  $A_0 = \text{constant}$ ,  $K = \text{constant}$ ,  $p_e = \text{constant}$ , as desired, while equating the first and last members in (3.21) we obtain that  $d\phi = 0$ , which gives  $\phi = \text{constant}$  across the  $\lambda_1$  wave. The second result is obtained from manipulating the first equality, leading to

$$\frac{c(A)}{A} dA + du = 0.$$

Integration in phase space gives

$$\int \frac{c(A)}{A} dA + u = \text{constant}.$$

The proof is completed.  $\square$

**Proposition 3.6.** The generalized Riemann invariants for  $\lambda_6 = u + c$  are

$$A_0 = \text{const}, \quad K = \text{const}, \quad p_e = \text{const}, \quad \phi = \text{const}, \quad \int \frac{c(A)}{A} dA - u = \text{const}. \quad (3.22)$$

*Proof.* The proof is entirely analogous to the previous case and is thus omitted.  $\square$

**Proposition 3.7.** The generalized Riemann invariants for  $\lambda_5 = u$  are

$$A_0 = \text{const}, \quad K = \text{const}, \quad p_e = \text{const}, \quad \phi \neq \text{const}, \quad A = \text{const}, \quad Au = \text{const}. \quad (3.23)$$

*Proof.* The proof is entirely analogous to the previous cases and is thus omitted.  $\square$

### 4 The Riemann problem

Here we pose and solve exactly the Riemann problem for the homogeneous version of system (3.9), that is the special Cauchy problem with piece-wise constant initial condition, namely

$$\begin{cases} \partial_t \mathbf{Q} + \mathbf{A}(\mathbf{Q}) \partial_x \mathbf{Q} = \mathbf{0}, & x \in \mathcal{R}, \quad t > 0, \\ \mathbf{Q}(x, 0) = \begin{cases} \mathbf{Q}_L, & \text{if } x < 0, \\ \mathbf{Q}_R, & \text{if } x > 0. \end{cases} \end{cases} \quad (4.1)$$

We seek the solution of the Riemann problem under the following constraints:

- fluid velocity  $u$  is smaller than the wave propagation speed  $c$ , so that for any  $\mathbf{Q}$ ,

$$\lambda_1(\mathbf{Q}) < 0 \quad \text{and} \quad \lambda_6(\mathbf{Q}) > 0; \quad (4.2)$$

- the cross sectional area of the vessel is bounded above and below, i.e.

$$0 < A_{\min} \leq A \leq A_{\max} < \infty. \quad (4.3)$$

Within the subsonic regime there are two possible wave configurations in the entire  $x-t$  half plane: configurations  $A$  and  $B$  which are depicted in Fig. 2.

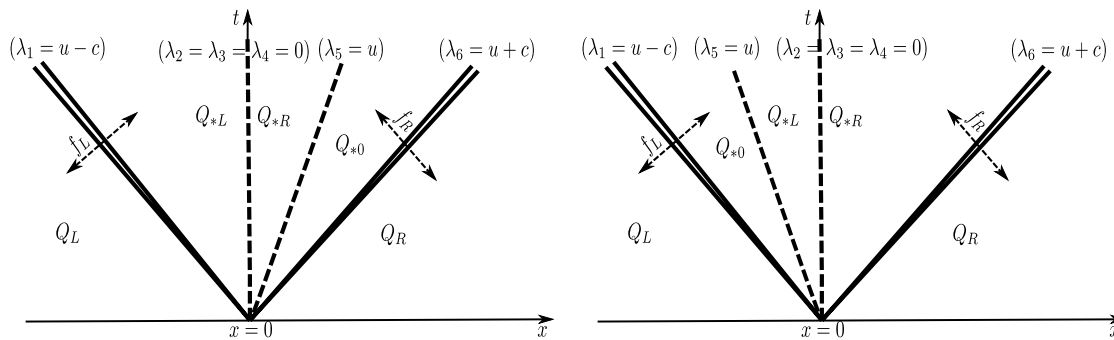


Figure 2: Structure of the solution of the Riemann problem (4.1) for the simplified  $6 \times 6$  blood flow model of this paper: configuration  $A$  (left), configuration  $B$  (right).

Each configuration is composed by six wave families. The left family is associated with the eigenvalue  $\lambda_1$ , the middle families are superimposed onto the  $t$ -axis, and are associated with  $\lambda_2$ ,  $\lambda_3$ , and  $\lambda_4$ . The other two families are associated respectively with  $\lambda_5$  and  $\lambda_6$ . Waves associated with the *genuinely non-linear* characteristic fields  $\lambda_1$  and  $\lambda_6$  are either shocks (discontinuous solutions) or rarefactions (smooth solutions), while the wave associated with the *linearly degenerate* characteristic fields  $\lambda_i$  ( $i=2, \dots, 5$ ) are contact discontinuities, the last one being a moving contact.

The entire solution consists of five constant states, namely  $\mathbf{Q}_L$  (data),  $\mathbf{Q}_{*L}$ ,  $\mathbf{Q}_{*R}$ ,  $\mathbf{Q}_{*0}$  and  $\mathbf{Q}_R$  (data), separated by four distinct waves. The unknown states to be found are  $\mathbf{Q}_{*L}$  (left of  $x=0$ ),  $\mathbf{Q}_{*R}$  (right of  $x=0$ ) and  $\mathbf{Q}_{*0}$ . The state  $\mathbf{Q}_{*0}$  lies between the moving contact and the nearest non-linear wave. See Fig. 2. If any of the  $\lambda_1$  and  $\lambda_6$  waves is a rarefaction then there will be a smooth transition between two adjacent constant states. In order to solve exactly the initial-value problem we need to establish appropriate jump conditions across each characteristic field to connect the unknown states  $\mathbf{Q}_{*L}$ ,  $\mathbf{Q}_{*R}$  and  $\mathbf{Q}_{*0}$  to the initial conditions  $\mathbf{Q}_L$  (left) and  $\mathbf{Q}_R$  (right). In what follows we establish such jump conditions across each characteristic field.

### 4.1 Jump across shocks: Rankine-Hugoniot conditions

An important feature of the proposed model for variable vessel properties is that the system cannot be expressed in conservation-law form. However, for the case of the Riemann problem the vessel properties  $h_0$ ,  $A_0$ ,  $E$ , (contained in  $K$ ), and thus  $p_e$  are constant across the non-linear waves. Hence, across the genuinely non-linear characteristic fields (rarefactions and shocks) it is possible to express the equations in conservation-law form. In fact it is sufficient to consider the reduced  $3 \times 3$  conservative system, excluding the equations for  $K$ ,  $A_0$  and  $p_e$  in (3.9). The homogeneous part of the equations in conservation-law form is

$$\partial_t \mathbf{Q} + \partial_x \mathbf{F}(\mathbf{Q}) = \mathbf{0}, \tag{4.4}$$

in terms of the redefined vector of conserved variables

$$\mathbf{Q} = \begin{bmatrix} q_1 \\ q_2 \\ q_3 \end{bmatrix} \equiv \begin{bmatrix} A \\ Au \\ A\phi \end{bmatrix} \tag{4.5}$$

and flux vector

$$\mathbf{F}(\mathbf{Q}) = \begin{bmatrix} f_1 \\ f_2 \\ f_3 \end{bmatrix} \equiv \begin{bmatrix} Au \\ Au^2 + \frac{KA}{\rho} \left( \frac{m}{m+1} \alpha^m - \frac{n}{n+1} \alpha^n \right) \\ \phi Au \end{bmatrix}. \tag{4.6}$$

**Proposition 4.1.** If the left  $\lambda_1$ -wave is a left-facing shock wave of speed  $S_L$  then

$$u_{*L} = u_L - f_L, \quad f_L = \sqrt{\frac{B_L(A_{*L} - A_L)}{A_L A_{*L}}}, \tag{4.7a}$$

$$B_L = \frac{K_L}{\rho} \left[ \frac{m}{m+1} \frac{A_{*L}^{m+1} - A_L^{m+1}}{A_0^m} - \frac{n}{n+1} \frac{A_{*L}^{n+1} - A_L^{n+1}}{A_0^n} \right], \tag{4.7b}$$

with

$$\phi_{*L} = \phi_L \tag{4.8}$$

and the shock speed is given as

$$S_L = u_L - \frac{M_L}{A_L}, \quad M_L = \sqrt{B_L \frac{A_{*L} A_L}{A_{*L} - A_L}}. \quad (4.9)$$

*Proof.* In Fig. 2 we illustrate the function  $f_L$  that connects the velocity  $u_{*L}$  to the left data state and the unknown  $A_{*L}$ . Let us assume that the left  $\lambda_1$ -wave is a left-facing shock wave of speed  $S_L$ . We need to establish relations across the shock, for which one uses standard techniques, see [32, 33]. We first transform the equations to a stationary frame via

$$\hat{u}_L = u_L - S_L, \quad \hat{u}_{*L} = u_{*L} - S_L. \quad (4.10)$$

Then the jump conditions become

$$\begin{cases} A_{*L} \hat{u}_{*L} = A_L \hat{u}_L, \\ A_{*L} \hat{u}_{*L}^2 + \frac{K_L A_{*L}}{\rho} \left( \frac{m}{m+1} \alpha_{*L}^m - \frac{n}{n+1} \alpha_{*L}^n \right) = A_L \hat{u}_L^2 + \frac{K_L A_L}{\rho} \left( \frac{m}{m+1} \alpha_L^m - \frac{n}{n+1} \alpha_L^n \right), \\ A_{*L} \hat{u}_{*L} \phi_{*L} = A_L \hat{u}_L \phi_L. \end{cases} \quad (4.11)$$

Now from the first equation in (4.11) define  $M_L = -A_{*L} \hat{u}_{*L} = -A_L \hat{u}_L$ . In fact this is the mass flux through the wave, which is constant. Use of  $M_L$  into the second equation in (4.11) followed by suitable manipulations leads to the sought relations (4.7). Details of the calculation of the shock speed  $S_L$  are omitted. From the first relation in (4.11) it follows that

$$\phi_{*L} = \phi_{*R}. \quad (4.12)$$

That is, the concentration is constant across the shock.  $\square$

**Proposition 4.2.** If the right  $\lambda_6$ -wave is a right-facing shock wave of speed  $S_R$  then

$$u_{*R} = u_R + f_R, \quad f_R = \sqrt{\frac{B_R (A_{*R} - A_R)}{A_R A_{*R}}}, \quad (4.13a)$$

$$B_R = \frac{K_R}{\rho} \left[ \frac{m}{m+1} \frac{A_{*R}^{m+1} - A_R^{m+1}}{A_0^m} - \frac{n}{n+1} \frac{A_{*R}^{n+1} - A_R^{n+1}}{A_0^n} \right] \quad (4.13b)$$

and the shock speed is given as

$$S_R = u_R + \frac{M_R}{A_R}, \quad M_R = \sqrt{B_R \frac{A_{*R} A_R}{A_{*R} - A_R}}. \quad (4.14)$$

*Proof.* The proof follows the same methodology as for a left shock and details are thus omitted.  $\square$

### 4.2 Jump conditions across rarefactions

It is possible to establish jump relations across rarefactions waves by means of generalized Riemann invariants introduced in Section 3.3.

**Proposition 4.3.** Across a left rarefaction wave associated with the characteristic field  $\lambda_1 = u - c$  the following relations hold

$$u_{*L} = u_L - f_L, \quad f_L = \int_{A_L}^{A_{*L}} \frac{c(A)}{A} dA. \tag{4.15}$$

*Proof.* From the left generalized Riemann invariants (3.20) we can write

$$\int_{A_L}^{A_{*L}} \frac{c(A)}{A} dA + u_{*L} = u_L,$$

from which we have (4.15). □

**Proposition 4.4.** Across a right rarefaction wave associated with the characteristic field  $\lambda_3 = u + c$  the following relations hold

$$u_{*R} = u_R + f_R, \quad f_R = \int_{A_R}^{A_{*R}} \frac{c(A)}{A} dA. \tag{4.16}$$

*Proof.* The proof uses the right generalized Riemann invariants (3.22) and is entirely analogous to the previous case. □

### 4.3 Solution inside rarefactions

**Proposition 4.5.** The solution at a point  $P = (\hat{x}, \hat{t})$  inside a left rarefaction is given by:

$$\mathbf{Q}_{Lfan} \equiv \begin{cases} u = \frac{\hat{x}}{\hat{t}} + c, \\ c = \sqrt{\frac{K_L}{\rho} \left[ m \left( \frac{A_{rar}}{A_{0L}} \right)^m - n \left( \frac{A_{rar}}{A_{0L}} \right)^n \right]}, \end{cases} \tag{4.17}$$

where  $A_{rar}$  is obtained by solving the following non-linear equation:

$$\frac{\hat{x}}{\hat{t}} + \int_{A_L}^{A_{rar}} \frac{c(A)}{A} dA = u_L. \tag{4.18}$$

*Proof.* To find the solution inside a left rarefaction we consider a point  $P = (\hat{x}, \hat{t})$  inside the wave and a characteristic joining the origin  $(0,0)$  and  $P = (\hat{x}, \hat{t})$ . The speed of the characteristic is:

$$u - c = \frac{dx}{dt} = \frac{\hat{x}}{\hat{t}}, \quad (4.19)$$

where  $u$  and  $c$  are unknown values at  $P$  of the particle velocity and celerity, respectively. Also, we can connect  $P$  to the left data state via the generalised Riemann invariant:

$$u + \int_{A_L}^{A_{rar}} \frac{c(A)}{A} dA = u_L. \quad (4.20)$$

The simultaneous solution of (4.19) and (4.20) gives the sought result.  $\square$

**Proposition 4.6.** The solution at a point  $P = (\hat{x}, \hat{t})$  inside a right rarefaction is given by:

$$\mathbf{Q}_{Rfan} \equiv \begin{cases} u = \frac{\hat{x}}{\hat{t}} - c, \\ c = \sqrt{\frac{K_R}{\rho} \left[ m \left( \frac{A_{rar}}{A_{0R}} \right)^m - n \left( \frac{A_{rar}}{A_{0R}} \right)^n \right]}, \end{cases} \quad (4.21)$$

where  $A_{rar}$  is obtained solving the following non-linear equation:

$$\frac{\hat{x}}{\hat{t}} - \int_{A_R}^{A_{rar}} \frac{c(A)}{A} dA = u_R. \quad (4.22)$$

*Proof.* The proof is completely analogous to the previous case.  $\square$

#### 4.4 Jump conditions across the stationary contacts

We wish to establish jump conditions across the stationary contact discontinuity associated with the eigenvalues  $\lambda_2 = \lambda_3 = \lambda_4 = 0$ . As stated earlier, for variable material properties it is not possible to express the equations in conservation-law form and therefore it is not possible to apply the classical Rankine-Hugoniot conditions. Thus to establish jump conditions we follow two alternative approaches, leading to identical results.

**Proposition 4.7.** Across the contact discontinuity the following relations hold

$$Au = \text{constant}, \quad \frac{1}{2}\rho u^2 + \psi + p_e = \text{constant}, \quad \phi = \text{constant} \quad (4.23)$$

leading to

$$A_{*L}u_{*L} = A_{*R}u_{*R}, \quad A_{*L}\phi_{*L} = A_{*R}\phi_{*R}, \quad \frac{1}{2}\rho u_{*L}^2 + \psi_{*L} = \frac{1}{2}\rho u_{*R}^2 + \psi_{*R}. \quad (4.24)$$

*Proof.* We first apply generalized Riemann invariants across the linearly degenerate fields. This approach was advocated by [11] to analyse the Baer-Nunziato equations for two-phase compressible flow, a well-known non-conservative system. We obtain

$$\frac{dA}{0} = \frac{d(Au)}{0} = \frac{dK}{1} = \frac{dA_0}{0} = \frac{dp_e}{-\psi_K} = \frac{dA\phi}{0}, \tag{4.25}$$

$$\frac{dA}{0} = \frac{d(Au)}{0} = \frac{dK}{0} = \frac{dA_0}{1} = \frac{dp_e}{-\psi_{A_0}} = \frac{dA\phi}{0}, \tag{4.26}$$

$$\frac{dA}{1} = \frac{d(Au)}{0} = \frac{dK}{0} = \frac{dA_0}{0} = \frac{dp_e}{\frac{\rho}{A}(u^2 - c^2)} = \frac{dA\phi}{\phi}. \tag{4.27}$$

The second member of the above equations states immediately that across the contact discontinuity  $d(Au) = 0$  and thus  $Au = \text{constant}$ , while equating the first with the last member in Eq. (4.27) gives that  $\phi = \text{constant}$ , proving two results in (4.23).

Relations (4.25) also state that across the stationary contact (see Fig. 2),  $K$  and  $p_e$  do change. Equating the third and fifth members in (4.25) gives

$$\psi_K dK + dp_e = 0. \tag{4.28}$$

Equating the fourth and fifth members in (4.26), we obtain

$$\psi_{A_0} dA_0 + dp_e = 0 \tag{4.29}$$

and equating the first and fifth members in Eq. (4.27), we get

$$\frac{\rho}{A}(u^2 - c^2)dA - dp_e = 0. \tag{4.30}$$

Using  $d(Au) = 0$  just proved and  $c^2 = \frac{A}{\rho}\psi_A$  from the definition of wave speed we may write

$$\rho u du + \psi_A dA + \psi_K dK = 0, \quad \rho u du + \psi_A dA + \psi_{A_0} dA_0 = 0, \quad \rho u du + \psi_A dA + dp_e = 0. \tag{4.31}$$

But  $\psi = \psi(A; A_0, K)$  and thus  $d\psi = \psi_A dA + \psi_K dK + \psi_{A_0} dA_0$ . Therefore combining all relations in (4.31) we obtain  $\rho u du + d\psi + dp_e = 0$ , which after integration gives the second sought result in (4.23).

Now we adopt the thin-layer approach advocated by [30], also used to analyse the Baer-Nunziato equations [5]. It is assumed that the transition layer containing the contact discontinuity is vanishingly thin and that the solution is smooth within the layer. Assuming the layer travels with constant speed  $S$  we define the independent variable

$$\xi = x - St, \quad S = \text{constant}, \tag{4.32}$$

which measures distance across the layer. We now study the governing equations locally. For any function  $G(x, t)$  we have

$$\frac{\partial G}{\partial x} = \frac{\partial G}{\partial \xi} \frac{\partial \xi}{\partial x}, \quad \frac{\partial G}{\partial t} = \frac{\partial G}{\partial \xi} \frac{\partial \xi}{\partial t}. \tag{4.33}$$

Then the continuity equation (2.1) gives

$$\frac{\partial A}{\partial \xi} \frac{\partial \xi}{\partial t} + \frac{\partial Au}{\partial \xi} \frac{\partial \xi}{\partial x} = 0, \quad (4.34)$$

or

$$d((u - S)A) = 0 \quad (4.35)$$

and thus with  $S = 0$  we obtain  $d(Au) = 0$ , which is the first sought result in (4.23). Analogous manipulations for the momentum equation give  $\frac{1}{2}\rho u^2 + \psi + p_e = \text{constant}$ , which is the second sought result in (4.23) and the result is thus proved.  $\square$

#### 4.5 Solution of Riemann problem

In Section 4 we have put in place all the necessary relations to obtain the Riemann problem solution in the Star Region (the constant region straddling the contact discontinuity path) and the procedure is embodied in the following proposition.

**Proposition 4.8.** The solution of the Riemann problem in the *Star Region* is given by the solution of the following non-linear system

$$\begin{cases} f_1(x_1, x_2) = x_2 - u_L + f_L(x_1) = 0, \\ f_2(x_1, x_2, x_3, x_4) = x_2 x_1 - x_4 x_3 = 0, \\ f_3(x_1, x_2, x_3, x_4) = \frac{1}{2}\rho(x_2^2 - x_4^2) + K_L \left[ \left( \frac{x_1}{A_{0L}} \right)^m - \left( \frac{x_1}{A_{0L}} \right)^n \right] \\ \quad - K_R \left[ \left( \frac{x_3}{A_{0R}} \right)^m - \left( \frac{x_3}{A_{0R}} \right)^n \right] + (p_{eL} - p_{eR}) = 0, \\ f_4(x_3, x_4) = x_4 - u_R - f_R(x_3) = 0, \end{cases} \quad (4.36)$$

where the four unknowns of the problem are

$$\mathbf{X} = [x_1, x_2, x_3, x_4] \equiv [A_{*L}, u_{*L}, A_{*R}, u_{*R}], \quad (4.37)$$

with

$$f_L(x_1) = \begin{cases} \sqrt{\frac{B_L(x_1 - A_L)}{A_L x_1}}, & \text{if } A_{*L} > A_L, \\ \int_{A_L}^{x_1} \frac{c(A)}{A} dA, & \text{if } A_{*L} \leq A_L, \end{cases} \quad (4.38)$$

$$f_R(x_3) = \begin{cases} \sqrt{\frac{B_R(x_3 - A_R)}{A_R x_3}}, & \text{if } A_{*R} > A_R, \\ \int_{A_R}^{x_3} \frac{c(A)}{A} dA, & \text{if } A_{*R} \leq A_R. \end{cases} \quad (4.39)$$

The wave speeds  $c_L$  and  $c_R$  are evaluated on the data according to (3.13). The constants  $K_L$  and  $K_R$  are evaluated on the data from (2.6).

*Proof.* The proof involves putting together the results stated previously. Details are omitted.  $\square$

**Remark 4.1** (The complete solution). The numerical solution of the non-linear system (4.36) gives the six unknowns in the *Star Region*. The rest of the solution follows by applying the wave relations studied in Section 4. At this point we remark that the non-linear system (4.36) is solved numerically using a standard Newton method. It may well be advisable to study this system in more detail, in order perhaps to identify potential multiple solutions at this stage.

## 5 Sample solutions

In this section we consider test problems for a straight tube characterised by constant external pressure  $p_e$ . We select four test problems that can be solved exactly using the exact solver presented in Section 4. The physiological parameters are chosen to correspond to physiological situations. In all cases we take a tube of length  $0.5\text{ m}$ , tube wall thickness  $h_0 = 3.0 \cdot 10^{-4}\text{ m}$ , radius and cross section area at rest  $R_{0ref} = 3.0 \cdot 10^{-3}\text{ m}$  and  $A_{0ref} = \pi R_{0ref}^2$ , Young's modulus  $E_{ref} = 3.0 \cdot 10^5\text{ N/m}^2$ , exponents for the tube law  $m = 10$  and  $n = -\frac{3}{2}$  and Poisson ratio  $\nu = \frac{1}{2}$ . The coefficient  $K$  is taken as

$$K_{ref} = \frac{E_{ref}}{12(1-\nu^2)} \left( \frac{h_{0ref}}{R_{0ref}} \right)^3, \quad (5.1)$$

while blood density is  $\rho = 1050\text{ kg/m}^3$ . Initial data is that for the Riemann problem and are given in Tables 1 and 2.

Table 3 shows the values of the exact solution in the *Star Region* for Tests 1, 2, 3 and 4, for the area  $A_{*L}$ ,  $A_{*R}$  and the particle velocity  $u_{*L}$ ,  $u_{*R}$ . These numbers can also be useful to test numerical methods.

Figs. 3 to 6 show the results obtained for the test cases considered. In each figure we display the profiles of vessel diameter, particle velocity, concentration  $\phi$ , pressure, speed index  $S = u/c$  and the resulting wave configuration in the space-time plane. Fig. 3 displays the solution for Test 1 at time  $t = 0.02\text{ s}$ . The structure of the solution is composed

Table 1: Left initial conditions for Test 1, 2, 3, 4 and 5.

<i>test</i>	$A_L [m^2]$	$u_L [m/s]$	$\phi_L$	$K_L$	$A_{0L} [m^2]$
1	$3.2 \cdot 10^{-5}$	0.1	1.0	$60 \times K_{ref}$	$A_{0ref}$
2	$2.9 \cdot 10^{-5}$	0.2	1.0	$K_{ref}$	$A_{0ref}$
3	$3.42 \cdot 10^{-5}$	0.5	1.0	$K_{ref}$	$A_{0ref}$
4	$3.1 \cdot 10^{-5}$	-0.2	1.0	$K_{ref}$	$A_{0ref}$
5	$3.2 \cdot 10^{-4}$	4.0	0.0	$K_{ref}$	$A_{0ref}$

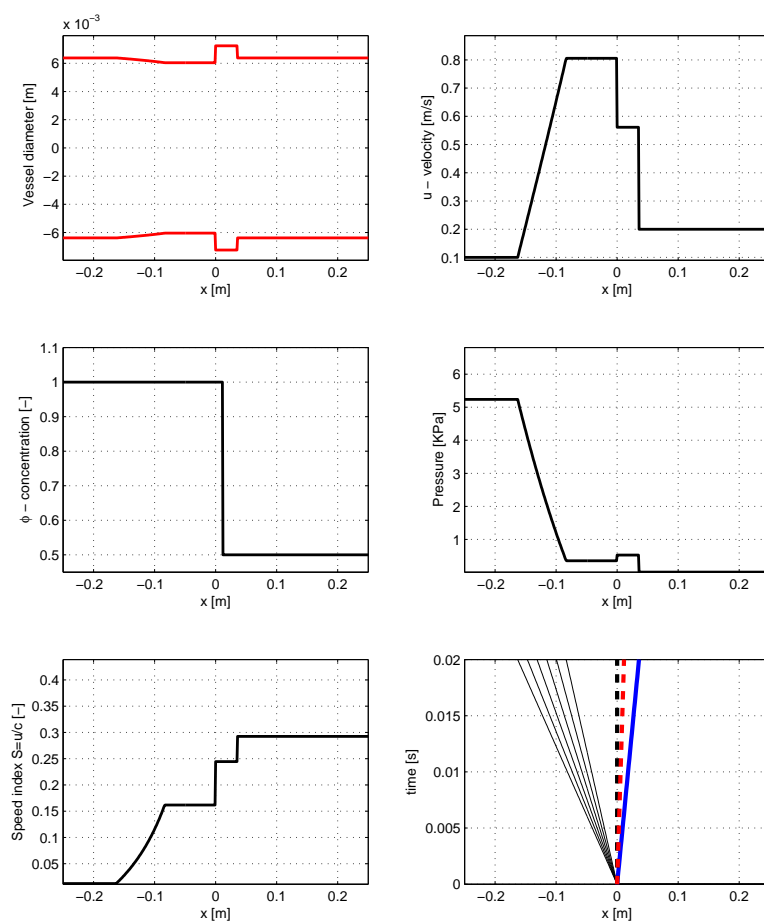


Figure 3: Exact solution of Test 1 at the output time 0.02 s.

by 6 waves: a left rarefaction associated to the wave family  $\lambda_1 = u - c$ ; three coincident contact discontinuities located at  $x = 0$  associated with the eigenvalues  $\lambda_2 = \lambda_3 = \lambda_4 = 0$ ; one contact discontinuity associated with  $\lambda_5 = u$  (see dashed line on the right-hand side of Fig. 3); a right shock wave associated with the wave family  $\lambda_6 = u + c$ .

Table 2: Right initial conditions for Test 1, 2, 3, 4 and 5.

test	$A_R [m^2]$	$u_R [m/s]$	$\phi_R$	$K_R$	$A_{0R} [m^2]$
1	$3.2 \cdot 10^{-5}$	0.2	0.5	$K_{ref}$	$1.1 \times A_{0ref}$
2	$3.2 \cdot 10^{-5}$	0.1	0.5	$100 \times K_{ref}$	$1.05 \times A_{0ref}$
3	$3.34 \cdot 10^{-5}$	-0.1	0.5	$40 \times K_{ref}$	$1.15 \times A_{0ref}$
4	$3.1 \cdot 10^{-5}$	0.1	0.5	$30 \times K_{ref}$	$1.05 \times A_{0ref}$
5	$1.1641 \cdot 10^{-4}$	0.4548	0.0	$K_{ref}$	$A_{0ref}$

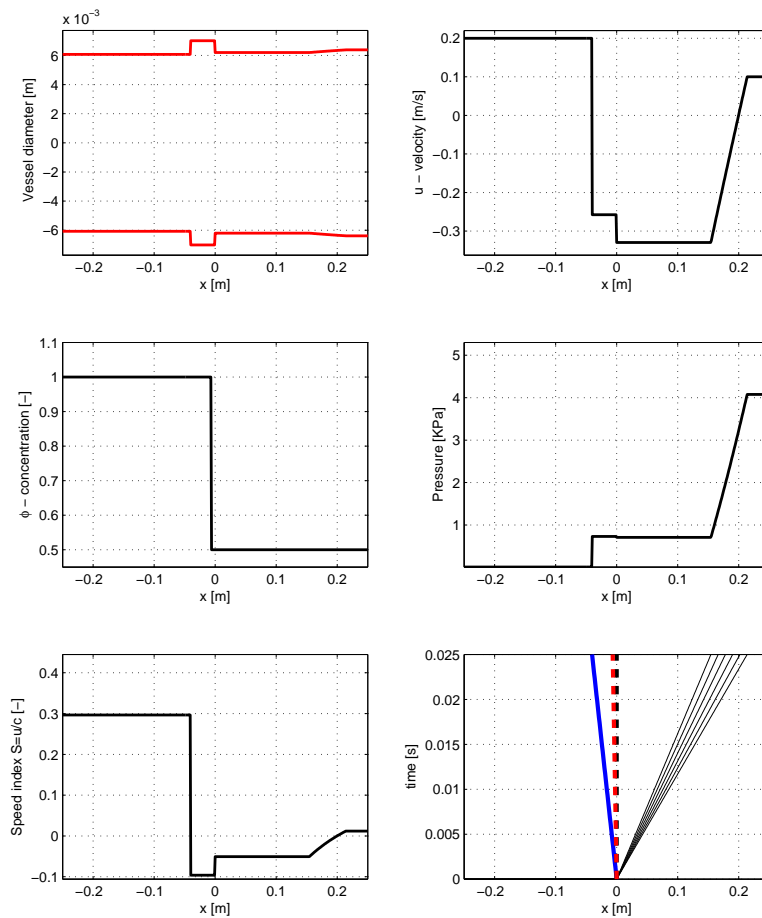


Figure 4: Exact solution of Test 2 at the output time 0.025 s.

Test 2 is the mirror image of Test 1 above. Fig. 4 shows the results at the output time  $t = 0.025$ s.

Fig. 5 shows results for Test 3 at time  $t = 0.05$ s. The solution includes two shock waves associated with the eigenvalues  $\lambda_1$  (left) and  $\lambda_6$  (right); three stationary contact waves associated with  $\lambda_2 = \lambda_3 = \lambda_4 = 0$ , located at  $x = 0$  and a right propagating contact wave

Table 3: Exact solution in the Star Region for Test 1, 2, 3, 4.

test	$A_{*L} [m^2]$	$u_{*L} [m/s]$	$A_{*R} [m^2]$	$u_{*R} [m/s]$
1	$2.8686 \cdot 10^{-5}$	0.8055	$4.1170 \cdot 10^{-5}$	0.5612
2	$3.8611 \cdot 10^{-5}$	-0.2577	$3.0202 \cdot 10^{-5}$	-0.3295
3	$4.0863 \cdot 10^{-5}$	0.0608	$3.4649 \cdot 10^{-5}$	0.0717
4	$2.5288 \cdot 10^{-5}$	-0.0767	$2.9616 \cdot 10^{-5}$	-0.0655

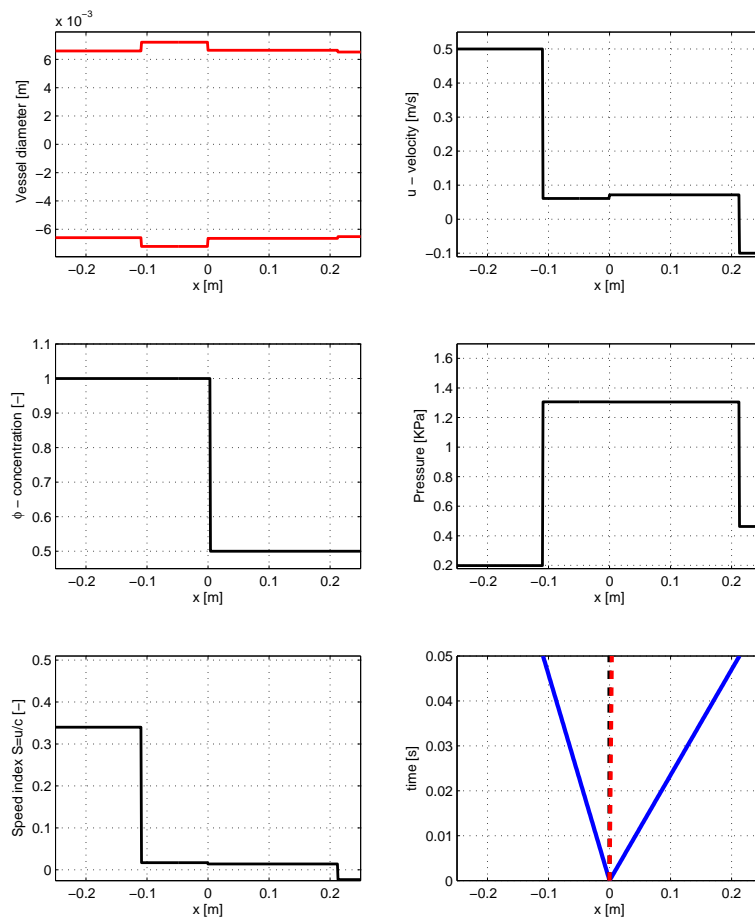


Figure 5: Exact solution of Test 3 at the output time 0.05 s.

associated with  $\lambda_5 = u$ .

Finally, Fig. 6 displays results for Test 4 at time  $t = 0.05$ s. The solution contains two rarefaction waves travelling in opposite directions associated with  $\lambda_1$  and  $\lambda_6$ . The rest of the wave pattern is composed by three stationary contact waves located at  $x = 0$  and associated with  $\lambda_2 = \lambda_3 = \lambda_4 = 0$  and a left propagating contact wave associated with  $\lambda_5$ .

## 6 Resonance and non-uniqueness

A drawback of our mathematical model for discontinuous material properties is the occurrence of *resonance and the loss of uniqueness*. Resonance happens when two or more eigenvalues coalesce, coupled with coincidence of eigenvectors and therefore losing hyperbolicity (weak hyperbolicity). Theoretical issues regarding resonance are found in the classical papers [19, 24] and references there in. For the hyperbolic system of this

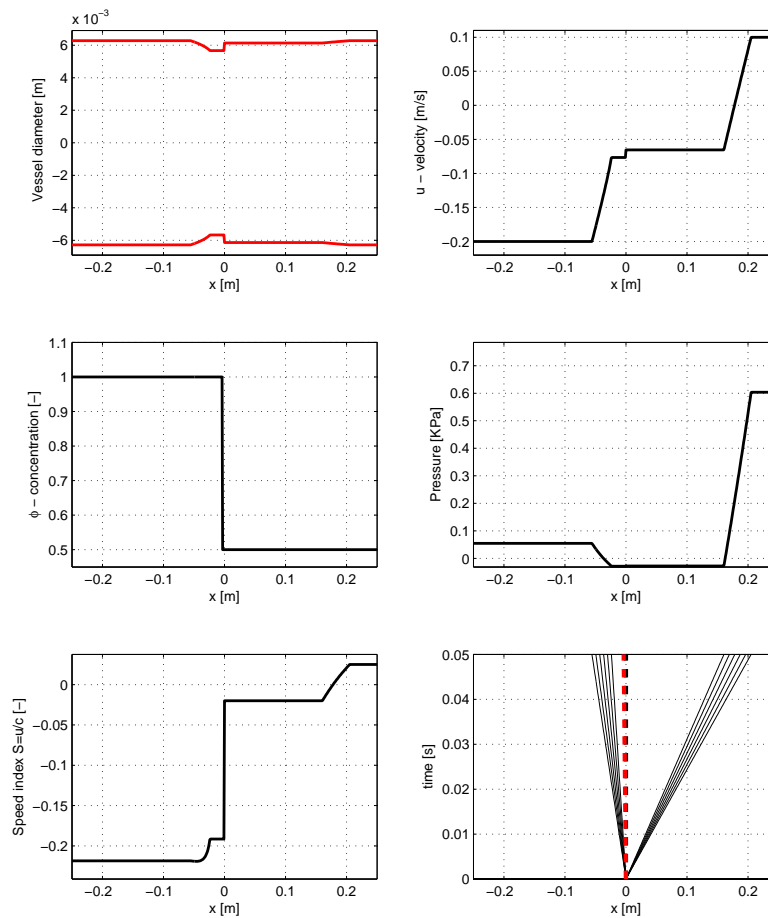


Figure 6: Exact solution of Test 4 at the output time 0.05 s.

paper, resonance takes place for critical flow associated with the  $\lambda_1$ -characteristic field, leading to  $\lambda_1 = \lambda_2 = \lambda_3 = \lambda_4 = 0$ . For critical flow associated with the  $\lambda_6$ -characteristic field we have  $\lambda_6 = \lambda_2 = \lambda_3 = \lambda_4 = 0$ . For other hyperbolic non-conservative systems there are at present a number of works worth mentioning. For example, for the augmented shallow water equations see [8, 26]. For a general hyperbolic system see the work [15]. To our knowledge, for our system (3.9) there is no published study available so far.

Just to illustrate the issue of non-uniqueness here we show a simple example. We consider the Riemann problem with initial condition as given in Tables 1 and 2 for Test 5. For this example we assume  $m = 1/2$ ,  $n = 0$  in the tube law (2.3)-(2.5).

Table 4 gives two solutions in the Star Region for the stated Riemann problem. Fig. 7 shows the complete wave pattern for one of the possible solutions; this is characterised by a left rarefaction associated with the eigenvalue  $\lambda_1$ . The rarefaction reaches the interface  $x = 0$  and from the interaction between the smooth wave and the stationary contacts a

Table 4: Test 5: two distinct solutions in the Star Region for the same initial conditions.

test	$A_{*L}[m^2]$	$u_{*L}[m/s]$	$A_{*R}[m^2]$	$u_{*R}[m/s]$	$A_*[m^2]$	$u_*$
Test 5: Solution 1	$3.8530 \cdot 10^{-4}$	3.0775	$2.1889 \cdot 10^{-4}$	5.4174	-	-
Test 5: Solution 2	$2.7776 \cdot 10^{-4}$	4.6735	$2.0229 \cdot 10^{-4}$	6.4171	$4.9899 \cdot 10^{-4}$	14.64

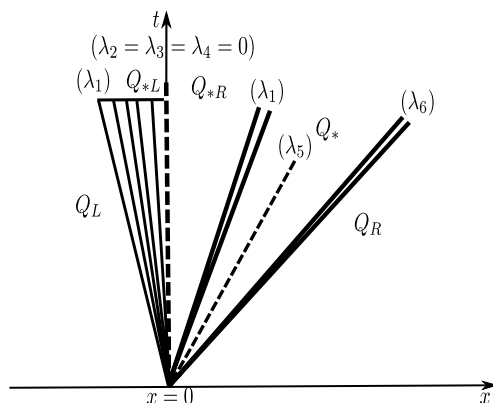


Figure 7: Structure of the solution of the Riemann problem in the resonant case for the  $6 \times 6$  blood flow model of this paper: configuration C.

new wave associated with the  $\lambda_1$ -characteristic field arises. This wave is followed by the  $\lambda_5$ - and  $\lambda_6$ -waves respectively.

The configuration given in Fig. 7 is typical of resonant hyperbolic systems as shown in [3,8,9,15].

The wave patterns depicted in Fig. 7 are found by solving the following non-linear system:

$$\left\{ \begin{array}{l} f_1(x_1, x_2) = x_2 - \sqrt{\frac{K_L}{\rho} \left[ m \left( \frac{x_1}{A_{0L}} \right)^m - n \left( \frac{x_1}{A_{0L}} \right)^n \right]} = 0, \\ f_2(x_1, x_2) = x_2 + \int_{A_L}^{x_1} \frac{c(A)}{A} dA - u_L = 0, \\ f_3(x_1, x_2, x_3, x_4) = x_2 x_1 - x_4 x_3 = 0, \\ f_4(x_1, x_2, x_3, x_4) = \frac{1}{2} \rho (x_2^2 - x_4^2) + K_L \left[ \left( \frac{x_1}{A_{0L}} \right)^m - \left( \frac{x_1}{A_{0L}} \right)^n \right] - K_R \left[ \left( \frac{x_3}{A_{0R}} \right)^m - \left( \frac{x_3}{A_{0R}} \right)^n \right] = 0, \\ f_5(x_3, x_4, x_5, x_6) = x_4 - x_6 - f_R(x_4, x_5) = 0, \\ f_6(x_5, x_6) = x_6 - u_R - f_R(x_5) = 0, \end{array} \right. \quad (6.1)$$

where the unknowns of the problem are

$$\mathbf{X} = [x_1, x_2, x_3, x_4, x_5, x_6] \equiv [A_{*L}, u_{*L}, A_{*R}, u_{*R}, A_*, u_*]. \quad (6.2)$$

The issue of admissibility criteria and identification of acceptable physical solutions is currently the subject of further studies by the authors and results will be published elsewhere.

## 7 Concluding remarks

A mathematical model for physiological flows in compliant vessels with discontinuous material properties has been presented. In particular, the equations could be used to model blood flow in veins. The equations have been thoroughly analysed and exact solutions have been constructed. These exact solutions can be useful for assessing the performance of numerical methods intended for practical applications by solving the general initial-boundary value problem. The given solutions, or approximations, can also be used locally to construct Godunov-type methods in the frameworks of finite volume methods and discontinuous Galerkin finite element methods. Work in progress includes a detailed study of the resonance and non-uniqueness phenomena and the implementation of suitable numerical methods for practical applications.

## Acknowledgments

This research has been partially funded by the Italian Ministry of University and Research (MIUR) under the project PRIN 2007.

## References

- [1] H. Akesson, M. Lindh, K. Ivancev, and B. Risberg. Venous stents in chronic iliac vein occlusions. *European Journal of vascular and endovascular surgery*, 13(3):334–336, 1997.
- [2] J. Alastruey, J. Parker, K. Peiro, S. Byrd, and S. Sherwin. Modelling the circle of Willis to assess the effects of anatomical variations and occlusions on cerebral flows. *Journal of Biomechanics*, 40:1794–1805, 2007.
- [3] F. Alcrudo and F. Benkhaldoun. Exact solutions to the Riemann problem of the shallow water equations with a bottom step. *Computers & Fluids*, 30(6):643–671, 2001.
- [4] N. Andrianov and G. Warnecke. On the solution to the Riemann problem for the compressible duct flow. *SIAM Journal on Applied Mathematics*, 64(3):878–901, 2004.
- [5] B. Asay, S. Son, and J. Bdzil. The role of gas permeation in convective burning. *International Journal of Multiphase Flow*, 23:923–952, 1996.
- [6] D. Beiko, B. Knudsen, and J. Denstedt. Reviews in endourology - Advances in ureteral stent design. *Journal of Endourology*, 17(4):195–199, 2003.
- [7] B. Brook, S. Falle, and T. Pedley. Numerical solutions for unsteady gravity-driven flows in collapsible tubes: evolution and roll-wave instability of a steady state. *Journal of Fluid Mechanics*, 396:223–256, 1999.
- [8] A. Chinnayya, A. L. Roux, and N. Seguin. A well-balanced numerical scheme for shallow-water equations with topography: resonance phenomena. *International Journal on Finite Volumes*, 2004.

- [9] S. Clain and D. Rochette. First- and second-order finite volume methods for the one-dimensional nonconservative Euler system. *Journal of Computational Physics*, 228(22):8214–8248, 2009.
- [10] D. Elad, R. Kamm, and A. Shapiro. Chocking phenomena in a lung-like model. *Journal of Biomechanical Engineering*, 109:1–92, 1987.
- [11] P. Embid and M. Baer. Mathematical analysis of a 2-phase continuum mixture theory. *Continuum Mechanics and Thermodynamics*, 4:4–279–312, 1992.
- [12] L. Formaggia, D. Lamponi, and A. Quarteroni. One-dimensional models for blood flow in arteries. *Journal of Engineering Mathematics*, 47:251–276, 2003.
- [13] M. Fullana and S. Zaleski. A branched one-dimensional model of vessel networks. *Journal of Fluid Mechanics*, 621:183–204, 2009.
- [14] Y.C. Fung. *Biomechanics: Circulation*, Second Edition. Springer Verlag, 1997.
- [15] P. Goatin and P.-G. LeFloch. The Riemann problem for a class of resonant hyperbolic systems of balance laws. *Annales de l’Institut Henry Poincaré-analyse non lineaire*, 21(6):881–902, 2004.
- [16] L. Gosse. A well-balanced flux-vector splitting scheme designed for hyperbolic systems of conservation laws with source terms. *Computers & Mathematics with Applications*, 39(9-10):135–159, 2000.
- [17] L. Gosse. A well-balanced scheme using non-conservative products designed for hyperbolic systems of conservation laws with source terms. *Mathematical Models & Methods in Applied Sciences*, 11(2):339–365, 2001.
- [18] J. Greenberg, A. LeRoux, R. Baraille, and A. Noussair. Analysis and Approximation of Conservation Laws with Source Terms. *SIAM Journal of Numerical Analysis*, 34:1980–2007, 1997.
- [19] E. Isaacson and B. Temple. Nonlinear resonance in systems of conservation-laws. *SIAM Journal of Applied Mathematics*, 52(5):1260–1278, 1992.
- [20] A. Jeffrey. *Quasilinear Hyperbolic Systems and Waves*. Pitman, 1976.
- [21] R. Kamm and A. Shapiro. Unsteady flow in a collapsible tube subjected to external pressure or body forces. *Journal of Fluid Mechanics*, 95:1–78, 1979.
- [22] P.G. LeFloch. Shock waves for nonlinear hyperbolic systems in nonconservative form. *Institute for Math. and its Appl., Minneapolis, IMA Preprint Series:593*, 1989.
- [23] R. LeVeque. Balancing Source Terms and Flux Gradients in High-Resolution Godunov Methods. *Journal of Computational Physics*, 146:346–365, 1998.
- [24] T. Liu. Nonlinear resonance for quasi-linear hyperbolic equation. *Journal of Mathematical Physics*, 28(11):2593–2602, 1987.
- [25] P. Moireau, N. Xiao, M. Astorino, C.A. Figueroa, D. Chapelle, C.A. Taylor, J.F. Gerbeau. External tissue support and fluid-structure simulation in blood flows. *Biomechanics and Modeling in Mechanobiology*, to appear, 2011.
- [26] A. Noussair. Riemann problem with nonlinear resonance effects and well-balanced Godunov scheme for shallow fluid past an obstacle. *SIAM Journal on Numerical Analysis*, 39(1):52–72, 2001.
- [27] C. Parés. Numerical Methods for Nonconservative Hyperbolic Systems: a Theoretical Framework. *SIAM Journal on Numerical Analysis*, 44:300–321, 2006.
- [28] T. J. Pedley. *The fluid dynamics of large blood vessels*, Third Edition. Cambridge University Press, 1980.
- [29] A. Quarteroni, M. Tuveri, and A. Veneziani. Computational vascular fluid dynamics: problems, models and methods. *Computing and Visualization in Science*, 2(4):163–97, 2000.

- [30] D. Schwendeman, C. Wahle, and A. Kapila. The Riemann Problem and a High-Resolution Godunov Method for a Model of Compressible Two-Phase Flow. *Journal of Computational Physics*, 212:490–526, 2006.
- [31] S. Sherwin, L. Formaggia, J. Peiro, and V. Franke. Computational modelling of 1D blood flow with variable mechanical properties and its application to the simulation of wave propagation in the human arterial system. *International Journal for Numerical Methods in Fluids*, 43:673–700,, 2003.
- [32] E. F. Toro. *Shock capturing methods for free surface shallow water flows*. Wiley and Sons, 2001.
- [33] E. F. Toro. *Riemann Solvers and Numerical Methods for Fluid Dynamics*, Third Edition. Springer-Verlag, 2009.
- [34] E. F. Toro and A. Siviglia. Simplified blood flow model with discontinuous vessel properties: analysis and exact solutions. In: *Modelling of Physiological Flows* (D. Ambrosi, A. Quarteroni, G. Rozza, Eds). Springer-Verlag, 2011.
- [35] T. Umscheid and W. Stelter. Time-related alterations in shape, position, and structure of self-expanding modular aortic stent grafts: a 4-year single-centre follow up. *Journal of Endovascular Surgery*, 6:17–32, 1999.
- [36] P. Zamboni, S. Lanzara, F. Mascoli, A. Caggiati, and A. Liboni. Inflammation in venous disease. *International Angiology, ProQuest Science Journals*, 27(5):361–369, 2008.